THERMAL BARRIER COATINGS FOR GAS TURBINE APPLICATIONS: FAILURE MECHANISMS AND KEY MICROSTRUCTURAL FEATURES

RECUBRIMIENTOS DE BARRERA TÉRMICA PARA APLICACIÓN EN TURBINAS A GAS: MECANISMOS DE FALLA Y PRINCIPALES CARACTERÍSTICAS MICROESTRUCTURALES

JULIAN D. OSORIO

Ms. C. Universidad Nacional de Colombia, Medellín, Colombia, jdosorio@unal.edu.co

ALEJANDRO TORO

Ph. D. Universidad Nacional de Colombia, Medellín, Colombia, aotoro@unal.edu.co

JUAN P. HERNÁNDEZ-ORTIZ

Ph. D. Universidad Nacional de Colombia, Medellín, Colombia, jphernandezo@unal.edu.co

Received for review April 30 th, 2012, accepted October 23th, 2012, final version November, 7 th, 2012

ABSTRACT: Advances in new materials for current power generation devices, such as gas turbines, have led to more efficient and durable engines that supply rising energy demands. High efficiencies in gas turbines, due to higher operating temperatures, have been accomplished through the development of thermal barrier coatings. These are multilayered systems that provide thermal isolation and protection against corrosion and high temperature erosion. In this work, we describe barrier application processes, their microstructural characteristics and their main failure mechanisms. Two different thermal barrier coatings are characterized and the latest trends of these systems are summarized.

KEYWORDS: Thermal Barrier Coating (TBC), Gas Turbine, Failure mechanisms

RESUMEN: Los avances en nuevos materiales para los dispositivos de generación de energía, como las turbinas a gas, han permitido incrementar su eficiencia y durabilidad para suplir la creciente demanda energética. Las altas eficiencias en las turbinas a gas como consecuencia de mayores temperaturas de operación, han sido posibles a través del desarrollo de recubrimientos de barrera térmica. Éstos son sistemas multicapas que proveen aislamiento térmico y protección contra la corrosión y erosión a alta temperatura. En este trabajo, se describe los procesos de aplicación de barreras térmicas, su microestructura y sus principales mecanismos de falla. Dos sistemas de barrera térmica son caracterizados y las nuevas tendencias de estos sistemas son resumidas.

PALABRAS CLAVE: Recubrimiento de Barrera Térmica (TBC), Turbina a gas, Mecanismos de falla

1. INTRODUCTION

Rising energy demands require development and design of novel technologies and materials. A high percentage of energy generation and transportation is done using gas turbines [1]. These have increased in efficiency due to protection systems such as the ceramic Top-Coat (TC) of Thermal Barrier Coatings (TBCs). TBCs provide thermal insulation for metallic components from combustion gases, allowing a reduction in the substrate temperature between 100 ºC to 300 ºC in 120 µm to 400 µm thicknesses [2-4]. In gas turbines, higher efficiencies are reached at higher operating temperatures [5-9] (see Figure 1). The TBCs have good mechanical properties and offer fracture and corrosion resistance at high temperatures [7-13].

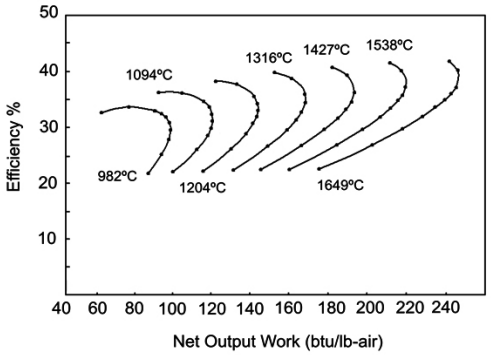

Figure 1. Efficiency increment in gas turbines with service temperatures [5].

As mentioned, developments of new materials for gas turbine manufacture are strongly connected with an increase in engine power, efficiency and durability. During the 1940s, the first Nickel-based superalloy was introduced for the aerospace industry. Since then, advanced materials, with excellent resistance to mechanical and chemical degradation at high temperatures, have become an important field of research and development. Every improvement in materials helped to increase operating temperatures and efficiencies of gas turbines. The first turbine blades were produced in the wrought form [1, 5, 14]; then induction vacuum casting technologies were developed during the 1950s, which significantly improved quality and cleanliness of the alloys. In the 1970s, casting with directional solidification enhanced fatigue life. By the 1990s, this technology allowed single-crystal blade production [1,14], which facilitated the removal of strengthening elements, such as boron and carbon, in order to reduce microsegregation and incipient melting during heat treatment [15]. At the same time, operating temperatures of the gas turbine were significantly increased thanks to the developments of TBCs. These new coatings were composed of zirconium dioxide, otherwise known as zirconia (ZrO_2), which exhibits a tetragonal phase at high temperatures. The tetragonal zirconia can be stabilized by the addition of Yttrium (Y^{+3}) which replaces a Zirconium (Zr^{+4}) in the lattice cell and forms Y_2O_3. It has been found that the tetragonal phase can be retained at room temperature with 6% to 8% of yttrium oxide (Y_2O_3) [16-18]. With these ceramic coatings, gas turbines reach temperatures ranging from 1400 °C to 1500 °C, above the superalloy's melting point (around 1300 °C) [1,15,19]. Figure 2 illustrates gas turbine operational temperatures as a function of materials development during the last decades [20]. Thus, whilst the primary role of the substrate is to bear mechanical loads and stresses developed during service, TBCs are designed to isolate and protect it against erosion and corrosion agents at high temperatures [15,19,21].

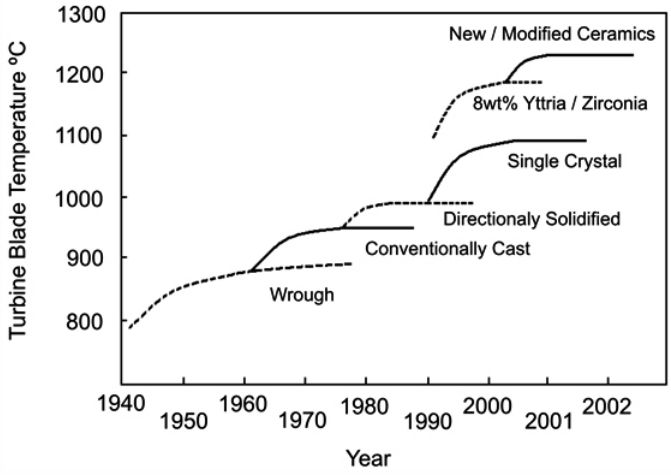

Figure 2. Chronological increase in operational temperature of turbine components [20].

Several processes have been used to deposit ceramic TCs of TBCs; the most relevant are Air Plasma Spray (APS) and Electron Beam Physical Vapor Deposition (EB-PVD). These processes provide ceramic coatings with excellent anchoring, thermal resistance and durability [12,20,22]. TBCs features and properties are a consequence of the deposition processes. In the APS process, the particles are injected into a plasma jet where they are heated until they melt or partially melt; they are then accelerated toward a metallic substrate. The drops impact the substrate and solidify, adopting the form of flattened disks known as splats [20,22,23]. The successive overlap of splats leads to a cross-sectional lamellar-like structure of the coating (see Fig. 3a), and cauliflower-like microstructure viewed from the top (see Fig. 3b). The final microstructure presents a high amount of elongated pores aligned perpendicularly to the heat flow, helping to reduce thermal conductivity [24,25]. In EB-PVD processes, an electron beam is used to vaporize an ingot of the coating material to produce a vapor cloud that is accelerated onto the substrate [15,23]. The resulting morphology of the coating consists of a series of columnar colonies that grow competitively in the cooling direction, normal to the surface of the substrate [26] (see Fig. 4).

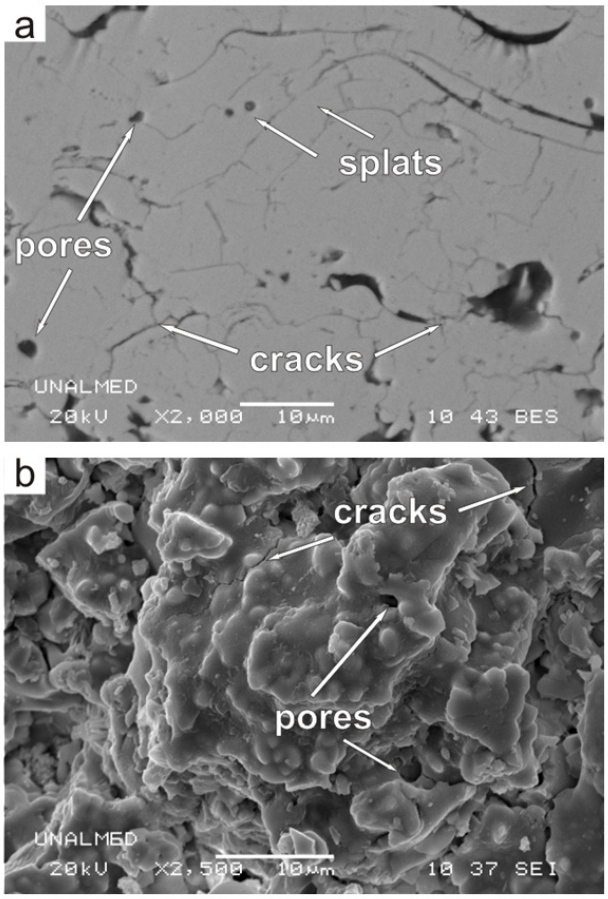

Figure 3. SEM micrographs of an Inconel 625 substrate's TC: a) cross-sectional view of a TC after 400 hours at 1100ºC; b) top-view of the TC after 200 hours at 1100ºC.

The thermal conductivity of APS-deposited TCs is significantly lower than that of EB-PVD coatings because of the differences in distribution and orientation of pores and cracks. A typical value of thermal conductivity in APS-deposited TCs is within the range of 0.8 w/m^{2}K to 1.7 w/m^{2}K [7,25]. In EB-PVD deposited TC, cracks and pores help reduce thermal conductivity to values between 1.5 w/m^{2}K to 2 w/m^{2}K. However, the columns are aligned parallel to the heat flux, directing heat transfer by conduction [7,25]. The durability of EB-PVD-deposited TC is higher compared with APS-deposited TC. The disconnected columns impart "strain tolerance" to the TC because they can separate at high temperatures, accommodating thermal expansion mismatch stresses [7,27]. The EB-PVD process is more expensive and less versatile than the APS process.

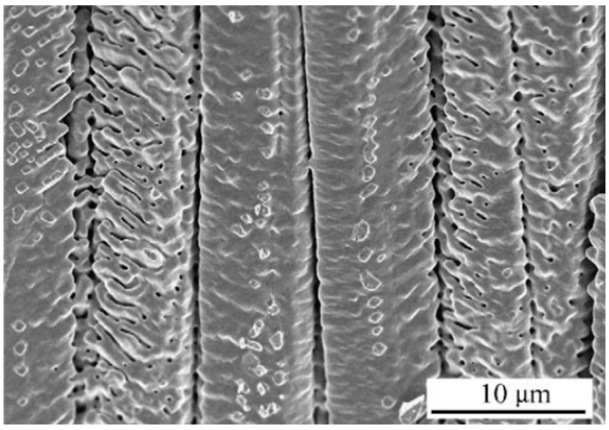

Figure 4. Cross-sectional image of a TBC applied by EB-PVD [26].

2. STRUCTURE OF A TBC SYSTEM

Conventional TBC systems consist of four materials: the Top-Coat (TC), the Bond-Coat (BC), the Thermally-Grown Oxide (TGO) layer and the substrate or Base Metal (BM). An Inconel 625 substrate with MCrAlY BC and APS-deposited $ZrO_2 - Y_2O_3$ TC was generated in order to analyze its microstructure and composition. The specimens were cut from a 30 cm x 30 cm plate using a precision saw cutting machine operating at 4000 rpm with a 1.2 mm/min feed-rate. The samples were treated at 1100ºC with exposure times between 1 and 1700 hours. SEM examination, and Energy-Dispersive X-ray Spectrometry (EDXS) microanalysis were carried out to identify and measure the elements present in the TC and TGO. Figure 5 shows an SEM micrograph of the TBC system on the Inconel 625.

The TC is a ceramic layer, usually yttria (Y_2O_3) stabilized zirconium oxide (ZrO_2), which interacts and faces combustion gases. As mentioned previously, it has been found that addition of 6 wt % to 8 wt % Y_2O_3 provides TCs with good thermal and mechanical properties [28-30]. We performed Wavelength-Dispersive X-ray Spectrometry (WDXS) to measure the chemical composition of the APS-deposited TC. The analysis gave 70.95 ± 0.37 wt % of Zr, 22.97 ± 0.28 wt % of O and 6.08 ± 0.27 wt % of Y [31]. An appreciable amount of yttrium (Y) was also detected, so a high stability of the tetragonal phase at room temperature is expected together with a lower TC thermal conductivity [28,32]. This effect can also be achieved with additions of other elements such as

hafnium (Hf) and some other earth oxides [16,33]. If no stabilizer elements are added, the ZrO_2 transforms to the monoclinic phase during cooling [28]. This phase is undesirable because it presents poor mechanical properties and it implies a volume change (around 5%), causing cracking and failure [12, 34-36].

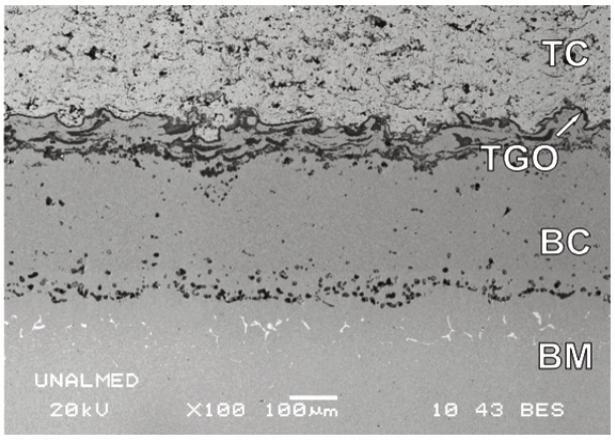

Figure 5. SEM cross-sectional view of a TBC system APS-deposited onto Inconel 625 substrate.

The TC is deposited onto the BC. There are two common types of BCs: Platinum-modified Nickel Aluminide (PtNiAl) and MCrAlY alloy where M refers to one or more of the elements Co, Ni and Fe. This layer provides adherence between the TGO and the substrate or between the TC and the substrate in the initial stages of the turbine's lifetime [37-39]. It contains 7 to 10 wt % of aluminum in order to form a protective oxide coating at the interface TC/BC. The TGO is a ceramic layer which forms as a consequence of Aluminum and Oxygen diffusion through the BC and the TC, respectively. This layer is mainly composed of α-Al_2O_3. In its initial stages, other phases can be formed, such as θ-Al_2O_3 and δ-Al_2O_3. These phases transform to stable α-Al_2O_3 at temperatures above 1000ºC [40-42]. The TGO is a fundamental layer because many failure mechanisms in the TBCs are related with its formation and growth [37,39,42-44]. It has been reported that the TGO critical thickness for TBC failure, by TC delamination, is between 5 and 6 µm [28,45,46].We predicted that the TGO thickness exhibits a power law dependence on time with an exponent of ½ [47] following the diffusion control mechanism of the TGO growth. To predict and analyze TGO growth, a one-dimensional diffusion-reaction equation was used, assuming constant diffusion coefficients for both the aluminum and oxygen. The system was solved numerically through a non-symmetrical Radial Basis Function (RBF) approach with a semi-implicit Finite Difference method (FDM) for the time derivatives [47]. The numerical results agree with the experimental measurements carried out in the thermally treated samples. In our experiments, the TGO thickness reaches the critical value of 5 µm after 600 hours of exposure at 1100ºC; however, no delamination was observed even after 1700 hours with a TGO thickness of 6.7 µm [31,47]. Figure 6 shows a transversal section image of the TGO acquired by Scanning Electron Microscopy (SEM).

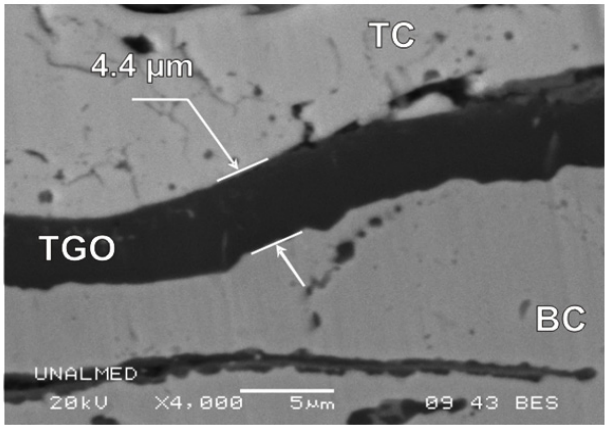

Figure 6. SEM Image of the TGO. The TBC was treated at 1100ºC during 200 hours

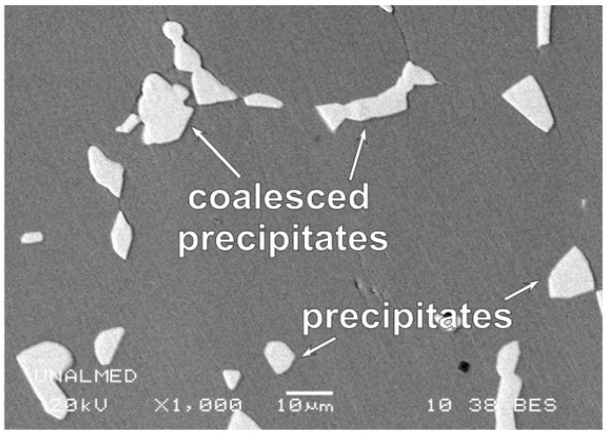

Figure 7. Mo and Cr-enriched Precipiates in a Inconel 625 matrix thermally treated during 1000 hours, 1100 ºC.

The TBC system is designed so that α-Al_2O_3 forms and grows slowly in order to become a barrier to the oxygen passage to the substrate. However, the growth of this

layer can generate stresses that, in combination with the BC/TC interfacial imperfections, are responsible for TBC failure [48-52]. It has been found that formation of α-Al_2O_3 is desirable because it provides good TC/BC adherence and exhibits a slower growth rate when compared with other oxides [42,50,53,54].

Table 1. Nominal composition and EDXS microanalysis of an Inconel 625 and an Hastelloy X substrates

%	Inconel 625	EDXS 1 wt-%	Hastelloy x	EDXS 2 wt-%
Ni	Balance	66.4	Balance	49.8
Mo	8.0 – 10.0	6.6	8.0 – 10.0	7.3
Cr	20.0 – 23.0	22.4	20.5 – 23.5	21.9
Fe	5.0 max	4.6	17.0 – 20.0	19.1
W	-	-	0.2 – 1.0	-
Co	-	-	0.5 – 2.5	0.6
Ti	0.4 max	-	-	-
Mn	-	-	1.0 max	0.8
C	0.10 max	-	0.05 – 0.15	-
Al	0.4 max	-	0.5 max	0.4
Nb+Ta	3.2 – 4.2	-	-	-

The last constituent of the system from the surface is the substrate, which is the structural component of the turbine. Many components exposed to high temperatures in gas turbines are manufactured using Ni-based superalloy substrates, typically Hastelloy X or Inconel 625. They offer good mechanical strength and excellent corrosion, oxidation and erosion resistances at high temperature [55,56]. These superalloys can contain significant amounts of alloying elements such as Cr, Mo, Al, Ti, Fe and C [15,57] and their microstructure is composed of highly stable austenite [15]. The addition of Aluminum and Titanium promotes the formation of intermetallic compounds such as Ni_3Al, Ni_3Ti and $Ni_3(Al,Ti)$ while Cr, Mo and C favor M_6C, $M_{23}C_6$ and M_7C_3-type carbide precipitation [57,58]. Figure 7 shows some Mo and Cr enriched precipitates in an Inconel 625 matrix after heat treatment at 1100 ºC during 1000 hours. It has been found that these precipitates improve the creep resistance of the superalloy because of their grain boundary pinning action [15]. Table 1 lists the EDXS microanalysis conducted in an Inconel 625 sample and a Hastelloy X sample extracted directly from a 7FA General Electric gas turbine combustion liner after an operation of 8000 hours (EDXS 1 for Inconel 625 and EDXS 2 for Hastelloy X); the nominal composition of the Inconel 625 and Hastelloy X [15,59] are also presented in the Table 1. For both cases, the compositional microanalyses present a good agreement with the respectively nominal compositions. However, the measured Mo content is slightly lower when compared with its nominal value. The Mo and Cr amounts are sufficient to promoted carbide precipitation as shown in Figure 7.

3. TBC'S FAILURE MECHANISMS

TBC systems are the main element of protection for gas turbines against the action of erosive agents at high temperatures. They can undergo thermal cycling and mechanical loads, which affect their performance, causing wear, cracks and TC delamination. Typical failure mechanisms in TBCs are associated with several factors such as chemical composition and TC microstructure. Failure is also affected by the TBC thermal and mechanical response to operating conditions: temperature, cycling time, combustion gasses, among others [48].

As mentioned before, TGO growth during operation is a consequence of aluminum and oxygen diffusion-reaction; this volumetric expansion can generate compressive stresses that favor cracking [7] and/or delamination when the thickness reaches a critical value [28,45,46]. During cooling, the thermal expansion mismatch between TGO and BC drives residual compressive stresses. They reach a maximum at room temperature and may lead to failure [7,60]. In addition, the compressive stresses developed during TGO growth, mainly under cycling conditions, cause TGO deformation [45,49,52] and contribute to its undulated shape (see Figs. 6 and 8). During the cycles, the localized penetration in the BC progresses and the downward displacements induce normal strains in the TBC. These strains form cracks that propagate laterally and eventually coalesce causing failure in one or both TGO interfaces [45,61,62]. This phenomenon is known as ratcheting.

The TBC is designed to develop a TGO constituted by α-Al_2O_3 (alumina) between the BC and TC. Nevertheless, other Ni, Cr and Al-enriched oxides such as $(Cr,Al)_2O_3$, $Ni(Cr,Al)_2O_4$ y NiO can appear.

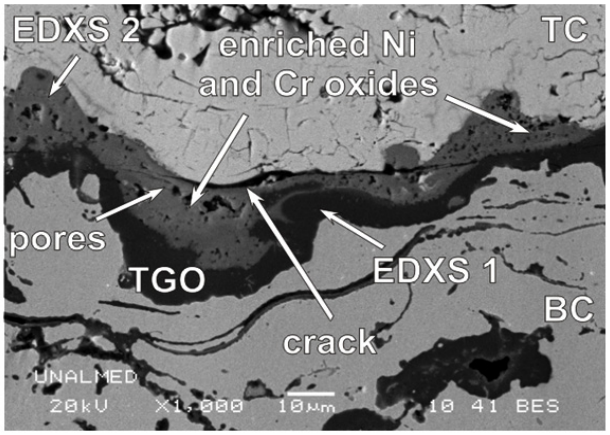

Figure 8. TGO, Ni, Cr-oxides SEM micrograph of the Inconel 625 substrate's TBC after a heat treatment at 1100ºC during 1000 hours.

Table 2. TGO chemical microanalysis

	EDXS 1 wt-%	EDXS 2 wt-%
Al	55.4	16.4
O	44.5	27.5
Cr	-	21.9
Ni	-	32.3
Y	-	1.9

Figure 8 shows a SEM micrograph of the TGO of a TBC with Inconel 625 substrate. In the figure, enriched Ni and Cr oxides are detected. Table 2 lists the EDXS microanalysis carried out in two regions of the TGO layer (EDXS 1 and EDXS 2), which is illustrated in Figure 8. The darker area (EDXS 1) corresponds to Al_2O_3 while the brighter area (EDXS 2) corresponds to Ni-, Cr-enriched oxides. These oxides are undesirable because they are porous, unstable and present a higher growth rate compared with alumina [46,63,64]. They induce tensile stresses that promote crack formation and propagation [51,65]. Some of these oxides can form at the initial stages of turbine lifetime before the TGO formation, due to compositional heterogeneities in the BC. Low aluminum concentration favors the stability of Ni and Cr-enriched oxides according to the ternary phase diagram presented in Fig. 9. Once the TGO is formed, diffusion of Al, Ni and Cr across the layer favor the formation of $(Cr,Al)_2O_3$, $Ni(Cr,Al)_2O_4$ y NiO in the TGO/TC interface [46,51,66]. It has been found that, after many hours at high temperatures, the alumina destabilizes and the following reactions to form chromium and nickel oxides may take place [51]:

$$Al_2O_3 + 2Cr \rightarrow Cr_2O_3 + 2Al, \quad (1)$$

$$Al_2O_3 + ½O2 + Ni \rightarrow NiAl_2O_4. \quad (2)$$

TBCs performance and durability are strongly influenced by their microstructure and how it changes during service. High porosity in TBC is a consequence of the application processes, resulting in desirable features such as higher strain tolerance and lower thermal conductivity. Therefore, it provides better insulation but leads to poorer mechanical properties of the coating [67-70]. During service, the TC undergoes a densification process, known as sintering, where crack healing increases splats' contact area and grain size; pores are redistributed and rounded leading to an increment in the thermal conductivity [25,71,72]. This change accelerates failure because higher conductivities imply higher temperatures, a reduction of thermal isolation and a faster TGO growth [73]. Sintering affects strain tolerance, decreasing system lifetime [69,70].

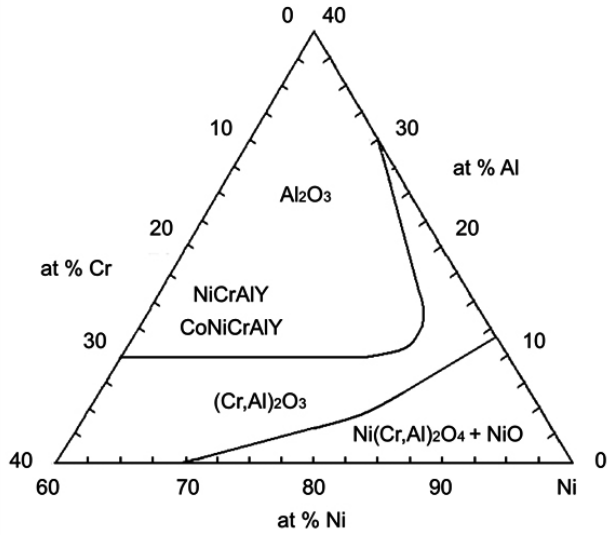

Figure 9. Ternary Phase diagram for Al, Cr and Ni [66].

Previous studies state that the sintering of ZrO_2 – Y_2O_3 coatings occurs in two stages [26,74]. The first stage is presented at short times with temperatures as low as 900ºC characterized by crack healing and grain growth. The second is a quasi-stationary stage in which pore shape changes to a spheroid-like aspect at temperatures higher than 1200ºC [75]. The effect of pore fraction on the thermal conductivity of an APS-deposited TC is shown in Fig. 10.

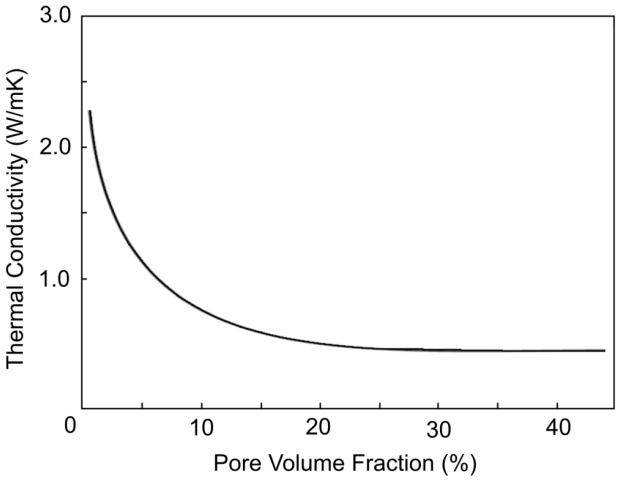

Figure 10. TC's thermal conductivity as a function of pore volume fraction [75].

4. FINAL REMARKS

Advances in TBCs are focused mainly on developments to improve efficiency and durability. To increase the efficiency through higher operation temperatures, materials with low thermal conductivity are being studied. Adding different rare earth ions as co-stabilizers has been effective to lower thermal conductivity, but the system exhibits an inferior lifetime compared to ZrO_2-6.8%Y_2O_3 [16,31]. Other oxides such as $Gd_2Zr_2O_7$ and $Sm_2Zr_2O_7$ present lower thermal conductivity than ZrO_2-6.8%Y_2O_3, but they are thermodynamically incompatible with alumina [19,28,33]. The main concern is to modify the ZrO_2-Y_2O_3 coating and develop a new layer with low thermal conductivity, thermodynamically compatible with alumina and with excellent mechanical properties.

Understanding TBC failure mechanisms is the basis to implement changes in order to improve durability. To maintain a strong bond between TC-TGO and TGO-BC, and also to reduce the magnitude of residual stresses close to these interfaces, intervention of BC composition, structure and processing can be accomplished [7,76]. It is important to ensure that a TGO composed only of α-Al_2O_3 forms and grows; Ni, Cr-enriched oxides reduce the fatigue strength of the coatings due to their effect on crack generation and propagation. There is evidence that the life of a coating is governed by the TGO thickening, which is in turn strongly influenced by the surface defects and roughness of the BC. Moreover, the failure of the system occurs when the TGO reaches a critical thickness [28]. To increase the system durability, efforts should be directed to reduce TGO growth rate [7], which can be accomplished by maximizing the grain size of the TGO [28], and developing coatings with lower thermal conductivity.

ACKNOWLEDGEMENTS

COLCIENCIAS and Empresas Públicas de Medellín (EPM) support this work through the co-funded project No 111845421942. The authors are grateful to the Material Characterization Laboratory at the Universidad Nacional de Colombia, Sede Medellín, for providing characterization instruments.

REFERENCES

[1] Reymann, H., MCrAlY Deposition by HVOF: A Suitable Alternative to LPPS. Turbine Forum: Advanced Coatings for High Temperatures, Nice Port St. Laurent, France, April, pp. 17-19, 2002.

[2] Vaidyanathan, K., Jordan, E. H. and Gell, M., Surface geometry and strain energy effects in the failure of a (Ni, Pt)Al/EB-PVD thermal barrier coating, Acta Mater., 52, pp. 1107–1115, 2004.

[3] Thompson, J. A. and Clyne, T. W., The effect of heat treatment on the stiffness of zirconia top coats in plasma-sprayed TBCs, Acta Mater., 49, pp. 1565–1575, 2001.

[4] Schlichting, K. W., Padture, N. P., Jordan, E. H. and Gell, M., Failure modes in plasma-sprayed thermal barrier coatings, Mater. Sci. Eng., A 342, pp. 120 – 130, 2003.

[5] Boyce, M. P., Gas Turbine Engineering Handbook, Gulf Professional Publishing, Second Edition, 2002.

[6] Jones, R. L., Reidy, R. F. and Mess, D., Scandia, yttria-stabilized zirconia for thermal barrier coatings, Surf. Coat. Tech., 82, pp. 70-76, 1996.

[7] Padture, N. P. and Jordan, H. E., Thermal Barrier Coatings for Gas-Turbine Engine Applications, Science 296, 280, 2002.

[8] Trice, R. W., Su, Y. J., Mawdsley, J. R. and Faber, K. T., Effect of heat treatment on phase stability, microstructure, and thermal conductivity of plasma-sprayed YSZ, J. Mater. Sci., 37, pp. 2359-2365, 2002.

[9] Sivakumar, R. and Mordike, B. L., High temperature

coatings for gas turbine blades: a review, Surf. Coat. Tech., 37, pp. 139 -160, 1989.

[10] Richard, C. S., Beranger, G., Lu, J. and Flavenot, J. F., The influences of heat treatments and interdiffusion on the adhesion of plasma-sprayed NiCrAlY coatings, Surf. Coat. Tech., 82, pp. 99-109, 1996.

[11] Kulkarni, A., Herman, H., Decarlo, F. and Subramanian, R., Microstructural Characterization of Electron Beam–Physical Vapor Deposition Thermal Barrier Coatings through High-Resolution Computed Microtomography, Metall. Mater. Trans. A., Volume 35A, 1945, 2004.

[12] Deng, H. X., Shi, H. J., Yu, H. C. and Zhong, B., Effect of heat treatment at 900°C on microstructural and mechanical properties of thermal barrier coatings, Surf. Coat. Tech., 205, pp. 3621–3630, 2011.

[13] González, A., López, E., Tamayo, A., Restrepo, E. and Hernández, F., Microstructure and Phases Analyses of Zirconia-Alumina (ZrO_2 - Al_2O_3) Coatings Produced By Thermal Spray. DYNA 77, Nro. 162, pp. 151-160, 2010.

[14] Hetmańczyk, M., Swadźba, L. and Mendala, B., Advanced materials and protective coatings in aero-engines application, J. Achieve. Mater. Manuf. Eng., Volume 24, Issue 1, 2007.

[15] Reed, R. C., The Superalloys: Fundamentals and Applications, Cambridge University Press, 2006.

[16] Winter, M. R. and Clarke, D. R., Thermal conductivity of yttria-stabilized zirconia–hafnia solid solutions, Acta Mater., 54, pp. 5051–5059, 2006.

[17] Ilavsky, J., Stalick, J. K. and Wallace, J., Thermal Spray Yttria-Stabilized Zirconia Phase Changes during Annealing, J. Therm. Spray Techn., Volume 10(3), 497, 2001.

[18] Krogstad, J. A., Lepple, M., Gao, Y., Lipkin, D. M. and Levi, C. G., Effect of Yttria Content on the Zirconia Unit Cell Parameters, J. Am. Ceram. Soc., 94 [12], pp. 4548–4555, 2011.

[19] Demasi-Marcin, J. T. and Gupta, D. K., Protective coatings in the gas turbine engine, Surf. Coat. Tech., 68/69, pp. 1–9, 1994.

[20] Sourmail, T., Coatings for high temperature applications, University of Cambridge, 2004. Available: http://Thomas-sourmail.net/coatings/index.html. [date 30 October 2012].

[21] Seadzba, L., et al. Erosion and corrosion resistant coatings for aircraft compressor blades, Surf. Coat. Tech., 62, pp. 486-492, 1993.

[22] Beele, W., Marijnissen, G. and Lieshout, A. V., The evolution of thermal barrier coatings status and upcoming solutions for today's key issues, Surf. Coat. Tech., 120–121, pp. 61–67, 1999.

[23] Xu, H. and Guo, H., Thermal barrier Coatings, Woodhead Publishing Limited, 2011.

[24] Adelpour, E., Thermal Barrier Coating for Gas Turbine Engine, Report University of California, San Diego. MAE 221A, 2007. Available: http://courses.ucsd.edu/rherz/mae221a/reports/adelpour_221A_F07.pdf. [date 30 October 2012].

[25] Hass, D. D., Slifka, A. J. and Wadley, H. N. G., Low thermal conductivity vapor deposited zirconia microstructures, Acta Mater., 49, pp. 973–983, 2001.

[26] Lughi, V., Tolpygo, V. K. and Clarke, D. R., Microstructural aspects of the sintering of the thermal barrier coatings, Mater. Sci. Eng., A 368, pp. 212 – 221, 2004.

[27] Strangman, T. E., Thermal Barrier Coatings for Turbine Airfoils, Thin Solid Films, 127, pp. 93-105, 1986.

[28] Clarke, D. R. and Levi, C. G., Materials design for the next generation thermal barrier coatings, Annu. Rev. Mater. Res. 33, pp. 383-417, 2003.

[29] Jones, R. L. and Reidy, R. F., Mess D. Scandia, yttria-stabilized zirconia for thermal barrier coatings, Surf. Coat. Tech., 82, pp. 70-76, 1996.

[30] Ballard, J. D., et al. Phase Stability of Thermal Barrier Coatings Made From 8 wt.% Yttria Stabilized Zirconia: A Technical Note, J. Therm. Spray Techn., 34, Volume 12(1), 2003.

[31] Osorio, J. D., Toro, A. and Hernández-Ortiz, J. P., Microstructure characterization of thermal barrier coating systems after controlled exposure to high temperature, submitted to J. Therm. Spray Techn., 2012.

[32] Winter, M. R. and Clarke, D. R., Oxide Materials with low Thermal Conductivity, J. Am. Ceram. Soc., 90, pp. 533–540, 2007.

[33] Zhu, D. and Miller, R. A., Development of Advanced Low Conductivity Thermal Barrier Coatings, Int. J. Appl. Ceram. Tec., 1 (1), pp. 86-94, 2004.

[34] Xie, L., Jordan, E. H., Padture, N. P. and Gell, M., Phase and microstructural stability of solution precursor plasma sprayed thermal barrier coatings, Mater. Sci. Eng. A, 381, pp. 189–195, 2004.

[35] Yoshikawa, N., Kikuchi, A., Taniguchi, S. and Takahashi, T., Tetragonal to monoclinic transformation in Y-TZP joined with metallic materials. J. Mater. Sci., 34, pp. 5885 – 589, 1999.

[36] Chambers, M. D. and Clarke, D. R., Effect of long term, high temperature aging on luminescence from Eu-doped YSZ thermal barrier coatings, Surf. Coat. Tech., 201, pp. 3942–3946, 2006.

[37] Nicoll, A. R. and Wahl, G., The effect of alloying additions on M-Cr-Al-Y Systems: an experimental study, Thin Solid Films, 95, pp. 21-34, 1982.

[38] Richard, C. S., Béanger, G., Lu, J. and Flavenot, J., F. The influences of heat treatments and interdiffusion on the adhesion of plasma-sprayed NiCrAlY coatings, Surf. Coat. Tech., 82, pp. 99-109, 1996.

[39] Smeggil, J. G., Some Comments on the Role of Yttrium in Protective Oxide Scale Adherence, Mater. Sci. Eng., 8-7, pp. 261-265, 1987.

[40] Doychak, J., Smialek, J. L. and Mitchel, T. E., 1989. In: Spitsberg, I. and Moreb, K., Effect of thermally grown oxide (TGO) microstructure on the durability of TBCs with PtNiAl diffusion bond coats, Mater. Sci. Eng. A, 417, pp. 322–333, 2006.

[41] Brickey, M. R. and LEE, J. L. Structural and Chemical Analyses of a Thermally Grown Oxide Scale in Thermal Barrier Coatings Containing a Platinum–Nickel–Aluminide Bondcoat, Oxid. Met., Vol. 54, Nos. 3/4, 2000.

[42] Reddy, A., et al. In Situ Study of Oxidation-Induced Growth Strains In a Model NiCrAlY Bond-Coat Alloy, Oxid. Met., Vol. 67, Nos. 3/4, 2007.

[43] Clarke, D. R., Christense, R. J. and Tolpygo, V., The evolution of oxidation stresses in zirconia thermal barrier coated superalloy leading to spallin failure, Surf. Coat. Tech., 94-95, 98-93, 1997.

[44] Karlsson, A. M., Hutchinson, J. W. and Evans, A. G., A fundamental model of cyclic instabilities in thermal barrier systems, J. Mech. Phys. Solids, 50, pp. 1565 – 1589, 2002.

[45] Spitsberg, I. and More, K., Effect of thermally grown oxide (TGO) microstructure on the durability of TBCs with PtNiAl diffusion bond coats, Mater. Sci. Eng. A, 417, pp. 322–333, 2006.

[46] Chen, W. R., Wu, X., Marple, B. R., Lima, R. S. and Patnaik, P. C., Pre-oxidation and TGO growth behaviour of an air-plasma-sprayed thermal barrier coating, Surf. Coat. Tech., 202, pp. 3787–3796, 2008.

[47] Osorio, J. D., Giraldo, J., Hernández, J. C., Toro, A. and Hernández-Ortiz, J. P., Diffusion-Reaction of Aluminum and Oxygen in Thermally Grown Al_2O_3 oxide layers, submitted to Heat Mass Transfer, 2012.

[48] Evans, A. G., Mumm, D. R., Hutchinson, J. W., Meier, G. E. and Pettit, F. S., Mechanisms controlling the durability of thermal barrier coatings, Prog. Mater. sci., 46, pp. 505-553, 2001.

[49] Nychka, J. A., Xu, T., Clarke, D. R. and Evans, A. G., The stresses and distortions caused by formation of a thermally grown alumina: comparison between measurements and simulations, Acta Mater., 52, pp. 2561–2568, 2004.

[50] Martena, M., et al. System failure: Stress distribution as a function of TGO thickness and thermal expansion mismatch, Eng. Fail. Anal., 13, pp. 409–426, 2006.

[51] Niranatlumpong, P., Ponton, C. B. and Evans, H. E., The Failure of Protective Oxides on Plasma-Sprayed NiCrAlY Overlay Coatings, Oxid. Met., Vol. 53, Nos. 3/4, 2000.

[52] Balint, D. S. and Hutchinson, J. W., An analytical model of rumplingin thermal barrier coatings, Journal of the Mechanics and Physics of solids, 53, pp. 949–973, 2005.

[53] Tolpygo, V. K., Clarke, D. R. and Murphy, K. S., Oxidation-induced failure of EB-PVD thermal barrier coatings, Surf. Coat. Tech., 146 –147, pp. 124–131, 2001.

[54] Hu, L., Hovis, D. B. and Heuer, A. H., Transient Oxidation of a C-Ni–28Cr–11Al Alloy, Oxid. Met., 73, pp. 275–288, 2010.

[55] Davis, J. R., Heat Resistant Materials (ASM Specialty Handbook). ASM International, 1997.

[56] Rai, S. K., et al. Characterization of microstructures in Inconel 625 using X-ray diffraction peak broadening and lattice parameter measurements, Scripta Mater., 51, pp. 59–63, 2004.

[57] Zhao, J. C., Larsen, M. and Ravikumar, V., Phase precipitation and time–temperature-transformation diagram of Hastelloy X, Mater. Sci. Eng. A, 293, pp. 112–119, 2000.

[58] Lee, T. H., Kim, S. J. and Jung, Y. C., Crystallographic Details of Precipitates in Fe-22Cr-21Ni-6Mo-(N) Superaustenitic Stainless Steels Aged at 900 8C, Metall. Mater. Trans. A, Volume 31a, 1713, 2000.

[59] ASTM B446. Standard Specification for Nickel-Chromium-Molybdenum-Columbium Alloy. 2008.

[60] Seo, D., et al. Influence of high-temperature creep stress on growth of thermally grown oxide in thermal barrier coatings, Surf. Coat. Tech., 203, pp. 1979–1983, 2009.

[61] Tolpygo, V. K. and Clarke, D. R., Rumpling of CVD (Ni,Pt)Al diffusion coatings under intermediate temperature cycling, Surf. Coat. Tech., 203, pp. 3278–3285, 2009.

[62] Tolpygo, V. K. and Clarke, D. R., Surface Rumpling of

a (Ni, Pt) Al Bond Coat Induced by Cyclic Oxidation, Acta mater., 48, pp. 3283-3293, 2000.

[63] Sohn, Y. H., Kim, J. H., Jordan, H. E. and Gell, M., Thermal cycling of EB-PVD - MCrAlY thermal barrier coatings: I. Microstructural development and spallation mechanisms, Surf. Coat. Tech., 146 –147, pp. 70–78, 2001.

[64] Nijdam, T. J., Jeurgens, L. P. H. and Sloof, W. G., Promoting exclusive α-Al_2O_3 growth upon high-temperature oxidation of NiCrAl alloys: experiment versus model predictions, Acta Mater., 53, pp. 1643–1653, 2005.

[65] Strawbridge, A., Evans, H. E. and Ponton, C. B., Spallation of oxide scales from NiCrAlY overlay coatings, Mater. Sci. Forum, Vols. 251-254, 365-372, 1997.

[66] Hindam, H. and Whittle, D. P., Microstructure, adhesion and growth kinetics of protective scales on metals and alloys, Oxid. Met., vol 18, 245, 1982.

[67] Cipitria, A., Golosnoy, I. O. and Clyne, T. A., sintering model for plasma-sprayed zirconia TBCs. Part I: Free-standing coatings, Acta Mater., 57, pp. 980–992, 2009.

[68] Deshpande, S., Kulkarni, A., Sampath, S. and Herman, H., Application of image analysis for characterization of porosity in thermal spray coatings and correlation with small angle neutron scattering, Surf. Coat. Tech., 187, pp. 6– 16, 2004.

[69] Siebert, B., Funke, C., Vaben, R. and Stöver, D., Changes in porosity and Young's Modulus due to sintering of plasma sprayed thermal barrier coatings, J. Mater. Process. Tech., 92-93, 217-223, 1999.

[70] Lu, X. J. and Xiao, P., Constrained sintering of YSZ/Al_2O_3 composite coatings on metal substrates produced from eletrophoretic deposition, J. Eur. Ceram. Soc., 27, pp. 2613–2621, 2007.

[71] Zhu, D. M. and Miller, R. A., Thermal conductivity and elastic modulus evolution of thermal barrier coatings under high heat flux conditions, J. Therm. Spray Techn., 9, 175, 2000.

[72] Zhu, D. and Miller, R. A., Thermal Conductivity Change Kinetics of Ceramic Thermal Barrier Coatings Determined by the Steady-State Laser Heat Flux Technique, NASA/TM, vol. 14, no. 1, pp. 146–141, 1999.

[73] Aaron, J. M., Chan, H. M., Harmer, M. P., Abpamano, M. and Caram, H. S., A phenomenological description of the rate of the aluminum/oxygen reaction in the reaction-bonding of alumina, J. Eur. Ceram. Soc., 25, pp. 3413–3425, 2005.

[74] Cernuschi, F., Lorenzoni, L., Ahmaniemi, S., Vuoristo, P. and Mäntylä, T., Studies of the sintering kinetics of thick thermal barrier coatings by thermal diffusivity measurements, J. Eur. Ceram. Soc., 25, pp. 393–400, 2005.

[75] Hass, D., Directed Vapor Deposition of thermal barrier coatings [PhD Thesis]. School of Engineering and Applied Science University of Virginia, 2001. Available: http://www.ipm.virginia.edu/research/PVD/Pubs/thesis6

[76] Spitsberg, I. T., Mumm, D. R. and Evans, A. G., On the failure mechanisms of thermal barrier coatings with diffusion aluminide bond coatings, Mater. Sci. Eng. A, 394, pp. 176–191, 2005.